

Proteomic shifts post-plasma cell therapy in AL amyloid plaques and potential implications for light chain-directed anti-fibril monoclonal antibodies

Systemic light-chain (AL) amyloidosis is caused by the production of immunoglobulin light chains which misfold and accumulate to cause tissue injury. Current treatments halt amyloid deposition through the removal of circulating amyloidogenic free light chains (FLC) without removing existing deposits. There is significant interest in anti-fibril monoclonal antibodies to remove amyloid plaques, with three phase III clinical trials underway (NCT04973137, NCT04504825, NCT04512235). Despite this, our understanding of amyloid tissue toxicity and plaque removal following anti-plasma cell therapy is limited. We investigated the proteomic changes occurring in bone marrow (BM) amyloid plaques after chemotherapy in AL amyloidosis.

The study, which is a retrospective study of newly diagnosed AL patients seen at Mayo Clinic between 2011-2023 was approved by Mayo Clinic's institutional review board. Patients were eligible if they had: (i) both a pre-treatment and post-treatment BM analysis performed at Mayo Clinic, Rochester, with identifiable Congo Red deposits; (ii) either a hematologic complete response or a very good partial response (responders); or (iii) a hematologic partial response or worse (non-responders) with ≥ 3 months of treatment at the time of the repeat BM. All samples were analyzed at the Mayo Proteomics Core and underwent laser microdissection followed by liquid chromatography and electrospray tandem mass spectrometry. Protein spectral counts, normalized to the total number of spectral counts per laser microdissection, were used as a semiquantitative measure of abundance. Differences in protein levels were expressed as \log_2 fold change, where a negative result indicates an increase in post-treatment samples and a positive result indicates an increase in pre-treatment samples. All identified proteins were considered part of the expanded amyloid proteome. Overrepresentation analyses were performed using WebGestalt reactome pathway database 2024; a false detection rate (FDR)-corrected $P < 0.05$ was used to identify significantly overrepresented pathways. Hematologic responses were graded according to consensus criteria.

Of 1,599 AL patients seen over the study period we identified 89 eligible cases and successfully analyzed paired samples from 63 patients (54 responders, 9 non-responders). A diagram illustrating how the experimental population was derived from the total Mayo Clinic Rochester AL amyloidosis population is provided in *Online Supplementary Figure S1*. Patients' baseline demographics, disease

characteristics, first-line treatment, and hematologic responses are summarized in Table 1. The median follow up was 4.3 years. The median age was 62 years and there was a male predominance (67%). Most patients had a λ isotype (76%), with a median difference between involved and uninvolved FLC (dFLC) at diagnosis of 15 mg/dL (interquartile range [IQR], 9-52) and BM plasma cell burden of 9% (IQR, 5-15). There were no significant differences in age, sex, light-chain isotype, dFLC, cardiac stage, or the use of autologous stem cell transplant between responders and non-responders. Fewer non-responders received daratumumab-containing regimens (11% vs. 26%), but the difference was not statistically significant ($P = 0.5$). The most common hematologic response at time of repeat BM among responders was a very good partial response (59%) and among non-responders was no response (56%). The median time between treatment initiation and repeat BM was 4 months (IQR, 3-9) for non-responders and 5 months (IQR, 4-9) for responders ($P = 0.8$). The histological amyloid burden quantified in pathology reports did not differ significantly between pre- and post-treatment samples. A summary of the best organ response obtained for eligible patients, stratified according to hematologic response at the time of repeat BM is shown in *Online Supplementary Table S1*.

We compared proteomic changes between pre- and post-treatment BM samples among responders: the differentially expressed protein pathways are shown in Figure 1A, B. Myosin, as well as early and terminal complement factors were over-represented in post-treatment samples. The former has been implicated in clathrin-mediated endocytosis of amyloid fibrils by non-immune cells, such as cardiomyocytes and mesangial cells, which could account for its presence in a non-muscle tissue.¹⁻³ Regarding the latter, a complete list of differentially expressed complement proteins among responders is presented in Table 2. As a key immunological effector system, complement has an established role in amyloid fibril opsonization and phagocytosis.³⁻⁵ However, an inflammatory response around amyloid deposits is not seen in humans, in contrast to mouse models which rapidly clear amyloidomas even in the absence of anti-fibril antibodies.⁶ Terminal complement components which contribute to membrane attack complex (MAC) formation are consistently associated with higher disease stage in cardiac (AL, ATTR) and renal (AL) amyloidosis,^{7,8} as well as a lower likelihood of achieving a renal organ response.⁵ As such, we hypothesize that

Table 1. Patients' demographics, disease characteristics, first-line treatment, and treatment response according to hematologic response category.

Characteristic	Non-responders N=9	Responders N=54	<i>P</i> *
Age, years, median (IQR)	60 (55-63)	62 (57-67)	0.3
Female, N (%)	3 (33)	18 (33)	>0.9
Lambda isotype, N (%)	5 (56)	43 (80)	0.2
Heavy chain involved, N (%)			0.2
No heavy chain	2 (22)	28 (52)	
IgG	5 (56)	19 (35)	
IgA	1 (11)	5 (9)	
IgM	1 (11)	1 (2)	
IgD	0 (0)	1 (2)	
Baseline dFLC, mg/dL, median (IQR)	12 (3-32)	16 (9-54)	0.3
Baseline BM plasma cell %, median (IQR)	8 (5-32)	9 (5-15)	0.4
FISH performed, N (%)	7 (78)	43 (80)	>0.9
t(11;14)	3 (43)	22 (51)	>0.9
Cardiac involvement, N (%)	1 (11)	28 (52)	0.031
Renal involvement, N (%)	4 (44)	37 (69)	0.3
Cardiac stage, N (%)			0.4
Stage I	6 (67)	19 (35)	
Stage II	2 (22)	23 (43)	
Stage IIIA	1 (11)	10 (19)	
Stage IIIB	0 (0)	2 (4)	
First-line treatment, N (%)			0.5
VCd	5 (56)	16 (30)	
ICd	0 (0)	12 (22)	
DaraVCd	1 (11)	10 (19)	
ASCT without induction therapy	2 (22)	7 (13)	
MelDex	0 (0)	2 (4)	
Dara only	0 (0)	2 (4)	
DaraVd	0 (0)	2 (4)	
BR	1 (11)	1 (2)	
Kd	0 (0)	1 (2)	
Vd	0 (0)	1 (2)	
Front-line ASCT, N (%)	6 (67)	26 (48)	0.5
Hematologic response at 2 nd BM, N (%)			<0.001
Complete response	0 (0)	21 (39)	
VGPR	0 (0)	32 (59)	
dFLC-PR	0 (0)	1 (2)	
Partial response	3 (33)	0 (0)	
No response	5 (56)	0 (0)	
Relapse	1 (11)	0 (0)	
Histological amyloid burden pre-treatment, N (%)			0.9
High	1 (11)	6 (11)	
Moderate	5 (56)	34 (63)	
Low	3 (33)	14 (26)	
Histological amyloid burden post-treatment, N (%)			0.5
High	1 (11)	2 (4)	
Moderate	5 (56)	34 (63)	
Low	3 (33)	18 (33)	

*Wilcoxon rank sum test; Fisher exact test. IQR: interquartile range; dFLC: difference between involved and uninvolved free light chains; BM: bone marrow; FISH: fluorescence *in situ* hybridization; V: bortezomib; C: cyclophosphamide; d: dexamethasone; I: ixazomib; Dara: daratumumab; ASCT: autologous stem cell transplant; Mel: melphalan; Dex: dexamethasone; B: bendamustine; R: rituximab; K: carfilzomib; VGPR: very good partial response; dFLC-PR: partial free light chain response.

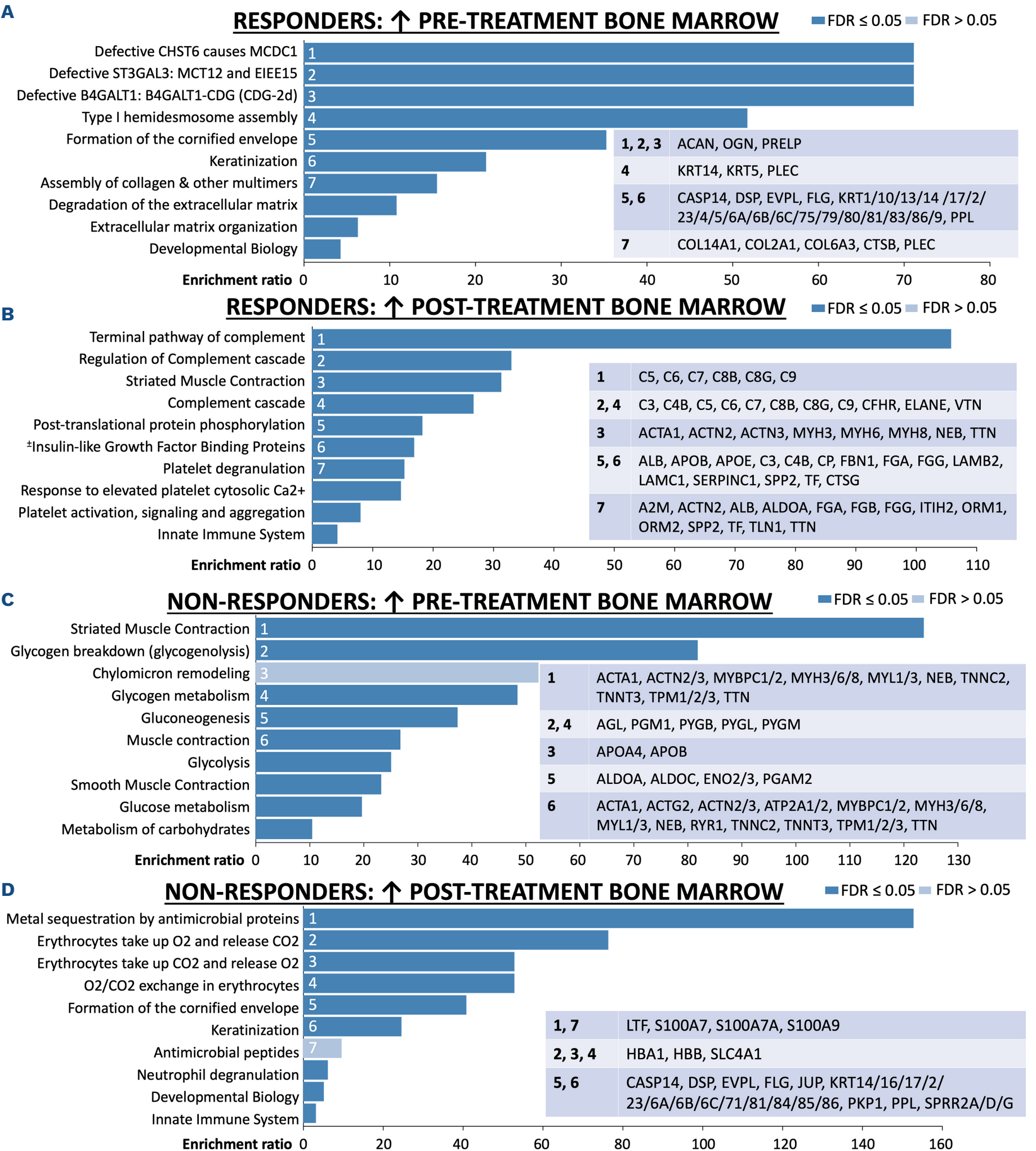


Figure 1. Pathway analyses (reactome) of proteins that were differentially expressed between pre-and post-treatment bone marrow samples. (A-D) Pathway analyses (reactome) of proteins that were differentially expressed between pre-and post-treatment bone marrow samples among responders (A, B), and non-responders (C, D) in AL amyloidosis. FDR: false discovery rate. (A) CHST6: carbohydrate sulfotransferase 6; MCDC1: mediator of DNA damage checkpoint 1; ST3GAL3: ST3 beta-galactoside alpha-2:3-sialyltransferase 3; MCT12: monocarboxylate transporter 12; EIEE15: early infantile epileptic encephalopathy 15; B4GALT1: beta-1:4-galactosyltransferase 1; B4GALT1-CDG: beta-1:4-galactosyltransferase 1 congenital disorder of glycosylation; ACAN: aggrecan; OGN: osteoglycin; PRELP: proline and arginine rich end leucine rich repeat protein; PLEC: plectin; CASP14: caspase 14; DSP: desmoplakin; EVPL: envoplakin; FLG: filaggrin; KRT1/5/10/13/14/17/2/23/4/ 5/6A/6B/6C/75/79/80/81/83/86/9: keratin

Continued on following page.

1/5/10/13/14/17/2 /23/4/5/6A/6B/6C/75/79/80/81/83/86/9; PPL: periplakin; COL14A1: collagen type XIV alpha 1 chain; COL2A1: collagen type II alpha 1 chain; COL6A3: collagen type VI alpha 3 chain; CTSB: cathepsin B. (B) C5: complement C5; C6: complement C6; C7: complement C7; C8B/G: complement C8 beta/gamma chain; C9: complement C9; C3: complement C3; C4B: complement C4B; C5: complement C5; CFHR: complement factor H related 5; ELANE: elastase: neutrophil expressed; VTN: vitronectin; ACTA1: actin alpha 1; ACTN2/3: actinin alpha 2/3; MYH3/6/8: myosin heavy chain 3/6/8; NEB: nebulin; TTN: titin; [†]Regulation of insulin-like growth factor transport and uptake by insulin-like growth factor binding proteins (IGFBP). (C) ACTA1: actin alpha 1; ACTN2/3: actinin alpha 2/3; MYBPC1/2: myosin binding protein C1/2; MYH3/6/8: myosin heavy chain 3/6/8; MYL1/3: myosin light chain 1/3; NEB: nebulin; TNNC2: troponin C2; TNNT3: troponin T3; TPM1/2/3: tropomyosin 1/2/3; TTN: titin; AGL: amylo-alpha-1:6-glucosidase: 4-alpha-glucanotransferase; PGM1: phosphoglucomutase 1; PYGB: glycogen phosphorylase B; PYGL: glycogen phosphorylase L; PYGM: glycogen phosphorylase: muscle associated; APOA4: apolipoprotein A4; APOB: apolipoprotein B; ALDOA: aldolase: fructose-bisphosphate A; ALDOC: aldolase: fructose-bisphosphate C; ENO2/3: enolase 2/3; PGAM2: phosphoglycerate mutase 2; ACTG2: actin gamma 2: smooth muscle; ATP2A1/2: ATPase sarcoplasmic/endoplasmic reticulum Ca²⁺ transporting 1/2; RYR1: ryanodine receptor 1. (D) LTF: lactotransferrin; S100A7: S100 calcium binding protein A7; S100A7A: S100 calcium binding protein A7A; S100A9: S100 calcium binding protein A9; HBA1: hemoglobin subunit alpha 1; HBB: hemoglobin subunit beta; SLC4A1: solute carrier family 4 member 1; CASP14: caspase 14; DSP: desmoplakin; EVPL: envoplakin; FLG: filaggrin; JUP: junction plakoglobin; KRT14/16/17/2/ 23/6A/6B/6C/71/81/84/85/86: keratin 14/16/17/2/ 23/6A/6B/6C/71/81/84/85/86; PKP1: plakophilin 1; PPL: periplakin; SPRR2A/D/G: small proline rich protein 2A/D/G.

the MAC could represent an excessive immune response which exacerbates tissue toxicity. Immunoglobulin-related proteins (IGKC, IGLC7, IGHG3, IGHG1, IGHG4, IGHG2) were all significantly reduced in post-treatment samples (*Online Supplementary Table S2*). This expected observation following the clearance of precursor FLC may reduce the antigenic burden available for the anti-fibril antibodies birtamimab and anselamimab to bind, thereby negatively impacting their efficacy. Anselamimab binds to a conformational epitope at the N-terminal on misfolded light chains, while birtamimab binds a highly conserved cryptic epitope exposed in misfolded light chains.^{9,10} Following opsonization, both antibodies induce macrophage-mediated phagocytosis of amyloid deposits.^{6,10} Indeed, it was recently announced that the phase III AFFIRM-AL trial examining birtamimab in patients with advanced cardiac amyloidosis was terminated after failing to meet either its primary endpoint of overall survival or key secondary endpoints.¹¹ The only immunoglobulin-related protein which increased after treatment among responders was IGLV3-21, which occurred at higher levels in two patients with λ FLC. The amyloid signature proteins apolipoprotein E, serum amyloid P (SAP) and vitronectin were significantly increased after treatment (Table 2). The only exception was a reduction in the amount of apolipoprotein A4 after treatment. Analogous to complement, the post-treatment increase in signature proteins may be a physiological attempt to opsonize amyloid deposits after FLC clearance, however, this may contribute to amyloid plaque persistence. Indeed, SAP protects amyloid deposits from degradation by phagocytic cells and proteolytic enzymes,¹² and SAP knock-out mice have a reduced severity of experimentally-induced amyloidosis.¹³ These findings may explain the persistence of amyloid deposits long-term and offers a mechanism for ongoing plaque-induced tissue toxicity (via complement activation). Irrespective of this, our findings indicate that immunoglobulin proteins are decreased after chemotherapy and alternative anti-fibrillar antibody targets, such as SAP, may be preferable.¹⁴ Nonetheless, a phase II study

of dezamizumab (an anti-SAP monoclonal antibody) did not consistently reduce left ventricular mass or improve cardiac function in treated patients.¹⁵ Potentially, limited cardiac uptake of dezamizumab, as demonstrated through the use of correlative immuno-positron emission tomography studies, could explain these results. Collagens, keratins and caspase 14 were enriched in diagnostic samples, suggesting a BM environment under cellular stress with associated fibrotic and apoptotic signaling. Keratinization has been associated with renal injury in AL, as keratins are released by nearby epithelial cells.^{8,16} We have also detected keratin proteins in amyloid plaques and tissue-wide samples of patients with advanced cardiac (AL, ATTR) amyloidosis, which suggests a preserved stress response to amyloid across sub-types and tissues.^{4,7} A comparison of proteins with the highest-fold increase in diagnostic and post-treatment BM samples among responders is shown in *Online Supplementary Table S3*. In diagnostic samples, proteins with the highest fold increase included structural extracellular proteins such as envoplakin, periplakin and aggrecan, while post-treatment samples were enriched for myosins, nebulins and creatine kinase, consistent with active tissue regeneration.

Protein pathways differentially expressed in BM samples from non-responders before and after treatment are shown in Figure 1C, D. Compared to responders, non-responders had no enrichment of complement protein pathways after treatment. However, other components of the innate immune system, including lactotransferrin, S100 calcium binding protein A7, A7A and A9, were increased.^{17,18} The pre-treatment samples of non-responders were also enriched for pathways involved in carbohydrate metabolism (AGL, PGM1, PYGB, PYGL, PYGM) and muscle contraction (actins, myosins) potentially suggesting greater levels of cellular activity in response to amyloid-induced cellular damage. Interestingly, keratins were significantly enriched after treatment among non-responders (compared to their enrichment in pre-treatment BM samples in responders). The explanation for this is unclear but may be related to

Table 2. Differential expression of complement-related proteins and amyloid signature proteins amongst responders in diagnostic and post-treatment bone marrow biopsy samples.

Gene	Protein name	Log ₂ fold change	FDR P
COMPLEMENT-RELATED PROTEINS			
C5	Complement C5	-0.8832	<0.0001
C6	Complement C6	-0.7166	<0.0001
CFHR5	Complement factor H-related protein 5	-0.6629	<0.001
C7	Complement C7	-0.5884	0.023
C8B	Complement C8 beta chain	-0.4419	0.013
C9	Complement C9	-0.3825	<0.0001
C8G	Complement C8 gamma chain	-0.3637	0.048
C4B	Complement C4-B	-0.2036	0.035
C3	Complement C3	-0.1863	<0.001
AMYLOID SIGNATURE PROTEINS			
APOE	Apolipoprotein E	-0.3758	<0.0001
APCS	Serum amyloid P-component	-0.1611	0.043
VTN	Vitronectin	-0.1587	0.0042
APOA4	Apolipoprotein A4	0.1498	0.00094

FDR: false discovery rate.

cellular stress or non-specific plaque adherence. Of signature proteins, there was only a significant reduction in apolipoprotein A4 (log₂fold-change=0.5738, FDR *P*<0.0001) in post-treatment samples, as was seen among the responders. In contrast, there was no significant enrichment in the other signature proteins after treatment. Regarding immunoglobulins, there was only a significant reduction in post-treatment samples for the immunoglobulin heavy chain μ (log₂fold-change=1.2726, FDR *P*=0.00021), possibly because of generalized immunoparesis secondary to chemotherapy. A comparison of proteins with the highest fold increase in pre- and post-treatment BM samples among non-responders is shown in *Online Supplementary Table S3*. Myosins and clathrin were present in pre- and post-treatment samples, suggesting clathrin-mediated endocytosis occurs independently of hematologic response. Another striking contrast was the relative abundance of insulin-degrading enzyme (IDE), which had the highest-fold increase in post-treatment BM samples from non-responders and the second highest fold increase in pre-treatment samples from responders. IDE promotes the degradation of amyloid plaques in Alzheimer disease, and its upregulation may be a homeostatic response to amyloid fibrils, with its relative abundance coinciding with the times of highest amyloid burden in the two groups.¹⁹ This study is subject to all the limitations inherent to a single-center retrospective review. Samples were identified based on availability and so may be subject to selection bias. Notably, we had a limited number of non-responder

samples relative to responders reflecting patterns of clinical practice, and limiting the generalizability of information regarding this group. Due to the period of the study there was significant variability in the treatments received. The histological assessment of amyloid burden is provided as a correlative finding only, given its semi-quantitative nature and lack of standardization. Despite the accuracy of laser microdissection, the risk of sample contamination from serum cannot be completely excluded. While protein quantitation was only semi-quantitative, the area of amyloid analyzed by laser microdissection-tandem mass spectrometry was standardized in each case, so only absolute rather than relative changes in protein content were detected. Nonetheless, this remains a methodological limitation which may adversely impact precise quantitative comparisons. The retrospective nature of this study means external validation is required. This is the first work to describe the changes which occur in the AL amyloid proteome following plasma cell therapy. While these findings are preliminary and require validation, the reduction in immunoglobulin proteins with effective treatments suggests that anti-fibril antibodies targeting alternate epitopes may be more effective in patients who have obtained a hematologic response. The increase of signature proteins following removal of immunoglobulin fragments suggests they may play a hitherto undescribed role in amyloid plaque stabilization, attaching to plaque binding points as these become available following treatment. Terminal complement proteins, such as the MAC,

appear to be a double-edged sword, potentially accelerating amyloid plaque removal albeit at the risk of excessive immunological activation and organ toxicity. Conceivably, signature protein opsonization of amyloid plaques after treatment may offset excessive complement activation by shielding immunologically reactive epitopes.

Authors

Matthew J. Rees,¹ Surendra Dasari,² Ellen D. McPhail,³ Angela Dispenzieri,¹ M. Cristine Charlesworth,⁴ Eli Muchtar,¹ Morie Gertz,¹ Navin Gupta,⁵ Emilie Anderson,¹ Samantha N. Quang,³ Christopher Dick,¹ Shaji Kumar¹ and Taxiarchis Kourelis¹

¹Division of Hematology; ²Department of Quantitative Health Sciences; ³Department of Laboratory Medicine and Pathology; ⁴Proteomics Core and ⁵Division of Nephrology, Mayo Clinic, Rochester, MN, USA

Correspondence:

M.J. REES - Rees.Matthew@mayo.edu

<https://doi.org/10.3324/haematol.2025.288217>

Received: May 9, 2025.

Accepted: July 11, 2025.

Early view: July 24, 2025.

©2026 Ferrata Storti Foundation

Published under a CC BY-NC license 

Disclosures

EM has provided consultancy services for Protego. AD has received

research funding from Pfizer, Janssen, Alnylam, Haemalogix, BMS, Alexion and Takeda and has provided consultancy services for BMS, Alexion and Takeda. MG has received honoraria from AstraZeneca, Alnylam: Ionis/Akcea, Medscape, Dava Oncology and Alexion; has received personal fees from AbbVie for participation in a Data Safety Monitoring board and has received personal fees from Sanofi, Janssen, Prothena and Johnson & Johnson. SK has received research funding from Sanofi, Roche, Novartis and Merck; has been a member of the Board of Directors and/or advisory committees for and received research funding from KITE, AbbVie, Celgene, Adaptive, Janssen, Takeda and MedImmune/AstraZeneca and has participated in an independent review committee for Oncopeptides. TK has received research funding from Pfizer and Novartis. The remaining authors have no conflicts of interest to disclose.

Contributions

MJR, SD and TK conceived and designed the study. AD, MCC, EM, MG, EA, CD and SK analyzed study material or data. MJR, EM, MCC, EA, SD and TK collected and assembled the data. MJR, SD and TK analyzed and interpreted the data. All authors gave final approval of the manuscript.

Funding

This work was supported by the Paul Calabresi K12 Career Development Award (CA90628–21), the Mayo Clinic Myeloma SPORE (P50CA186781) and the Ted and Loretta Rogers Cardiovascular Career Development Award Honoring Hugh C. Smith, M.D.

Data-sharing statement

Original data will be shared upon reasonable request. Please contact kourelis.taxiarchis@mayo.edu

References

- Cheng J, Grassart A, Drubin DG. Myosin 1E coordinates actin assembly and cargo trafficking during clathrin-mediated endocytosis. *Mol Biol Cell*. 2012;23(15):2891-2904.
- Teng J, Russell WJ, Gu X, Cardelli J, Jones ML, Herrera GA. Different types of glomerulopathic light chains interact with mesangial cells using a common receptor but exhibit different intracellular trafficking patterns. *Lab Invest*. 2004;84(4):440-451.
- Jordan TL, Maar K, Redhage KR, et al. Light chain amyloidosis induced inflammatory changes in cardiomyocytes and adipose-derived mesenchymal stromal cells. *Leukemia*. 2020;34(5):1383-1393.
- Kourelis TV, Dasari SS, Dispenzieri A, et al. A proteomic atlas of cardiac amyloid plaques. *JACC CardioOncol*. 2020;2(4):632-643.
- Rees MJ, Muchtar E, Atallah-Yunes SA, et al. Proteomic determinants of renal organ response in light-chain amyloidosis. *Amyloid*. 2025;32(2):200-202.
- Hrncic R, Wall J, Wolfenbarger DA, et al. Antibody-mediated resolution of light chain-associated amyloid deposits. *Am J Pathol*. 2000;157(4):1239-1246.
- Netzel BC, Charlesworth MC, Johnson KL, et al. Whole tissue proteomic analyses of cardiac ATTR and AL unveil mechanisms of tissue damage. *Amyloid*. 2025;32(1):72-80.
- Charalampous C, Dasari S, McPhail E, et al. A proteomic atlas of kidney amyloidosis provides insights into disease pathogenesis. *Kidney Int*. 2024;105(3):484-495.
- O’Nuallain B, Allen A, Kennel SJ, Weiss DT, Solomon A, Wall JS. Localization of a conformational epitope common to non-native and fibrillar immunoglobulin light chains. *Biochemistry*. 2007;46(5):1240-1247.
- Renz M, Torres R, Dolan PJ, et al. 2A4 binds soluble and insoluble light chain aggregates from AL amyloidosis patients and promotes clearance of amyloid deposits by phagocytosis. *Amyloid*. 2016;23(3):168-177.
- Prothena Corporation plc. Prothena Announces Phase 3 AFFIRM-AL Clinical Trial for Birtamimab in Patients with AL Amyloidosis Did Not Meet Primary Endpoint. In: Bachner M, ed. https://s201.q4cdn.com/351053094/files/doc_news/Prothena-Announces-Phase-3-AFFIRM-AL-Clinical-Trial-for-Birtamimab-

- in-Patients-with-AL-Amyloidosis-Did-Not-Meet-Primary-Endpoint-2025.pdf Accessed June 10, 2025.
12. Tennent GA, Lovat LB, Pepys MB. Serum amyloid P component prevents proteolysis of the amyloid fibrils of Alzheimer disease and systemic amyloidosis. *Proc Natl Acad Sci U S A*. 1995;92(10):4299-4303.
 13. Botto M, Hawkins PN, Bickerstaff MC, et al. Amyloid deposition is delayed in mice with targeted deletion of the serum amyloid P component gene. *Nat Med*. 1997;3(8):855-859.
 14. Wall J, Klein M, Guthrie S, et al. The peptide fusion immunoglobulin, AT-02, exhibits highly potent pan-amyloid reactivity and immunomodulation. *J Card Fail*. 2024;30(1):210.
 15. Wechalekar A, Antoni G, Al Azzam W, et al. Pharmacodynamic evaluation and safety assessment of treatment with antibodies to serum amyloid P component in patients with cardiac amyloidosis: an open-label phase 2 study and an adjunctive immuno-PET imaging study. *BMC Cardiovasc Disord*. 2022;22(1):49.
 16. Djudjaj S, Papasotiriou M, Bülow RD, et al. Keratins are novel markers of renal epithelial cell injury. *Kidney Int*. 2016;89(4):792-808.
 17. Kell DB, Heyden EL, Pretorius E. The biology of lactoferrin, an iron-binding protein that can help defend against viruses and bacteria. *Front Immunol*. 2020;11:1221.
 18. Singh P, Ali SA. Multifunctional role of S100 protein family in the immune system: an update. *Cells*. 2022;11(15):2274.
 19. Tian Y, Jing G, Zhang M. Insulin-degrading enzyme: roles and pathways in ameliorating cognitive impairment associated with Alzheimer's disease and diabetes. *Ageing Res Rev*. 2023;90:101999.